Morphology, structure and chemistry of extracted diesel soot—Part I: Transmission electron microscopy, Raman spectroscopy, X-ray photoelectron spectroscopy and synchrotron X-ray di...

ARTICLE *in* TRIBOLOGY INTERNATIONAL · AUGUST 2012

Impact Factor: 1.94 · DOI: 10.1016/j.triboint.2012.03.004

4 AUTHORS, INCLUDING:

Cristy Leonor Azanza Ricardo
Università degli Studi di Trento
36 PUBLICATIONS **269** CITATIONS
SEE PROFILE

P. Scardi
Università degli Studi di Trento
329 PUBLICATIONS **4,693** CITATIONS
SEE PROFILE

Pranesh Aswath
University of Texas at Arlington
110 PUBLICATIONS **1,052** CITATIONS
SEE PROFILE

Tribology International 52 (2012) 29–39

Contents lists available at SciVerse ScienceDirect

Tribology International

journal homepage: www.elsevier.com/locate/triboint

Morphology, structure and chemistry of extracted diesel soot—Part I: Transmission electron microscopy, Raman spectroscopy, X-ray photoelectron spectroscopy and synchrotron X-ray diffraction study

Mihir Patel [a], Cristy Leonor Azanza Ricardo [b], Paolo Scardi [b], Pranesh B. Aswath [a,*]

[a] Materials Science and Engineering Department, University of Texas at Arlington, Arlington, TX 76019, USA
[b] Department of Materials and Industrial Technology, University of Trento, Trento, Italy

ARTICLE INFO

Article history:
Received 27 September 2011
Received in revised form
6 March 2012
Accepted 9 March 2012
Available online 29 March 2012

Keywords:
Diesel soot
Synchrotron X-ray diffraction
Lubrication
Exhaust gas recirculation soot

ABSTRACT

Inclusion of soot in lubricating oil can result in increased wear and decreased lubricity. In this study we have attempted to gain fundamental insight into the morphology, structure and chemistry of diesel soot. Energy dispersive spectroscopy using TEM suggests interaction between lubrication additives and crankcase soot resulting in the presence of C, Ca, S, P, O and Zn. Synchrotron X-ray diffraction indicates the presence of different sulfates of calcium as well as the presence of amorphous zinc based compounds. Raman spectroscopy and selected area diffraction using TEM indicates that the turbostratic structures of the carbon in both are very similar.

1. Introduction

Exhaust Gas Recirculation (EGR) is one of the most effective post combustion protocols that heavy-duty diesel engine manufacturers have adopted as an effort to reduce emission of NOx and to comply with stringent emission norms API CJ 4 imposed by the Environmental Protection Agency (EPA) [1,2]. One of the undesirable effects of EGR is the accumulation of soot and transfer of highly reactive acidic materials to crankcase oil resulting in increased wear of power train components, piston cylinder and piston rings [3,4]. This puts increasingly greater stress on the functionality of lubrication oil to handle soot accumulation and adverse effect of corrosive products transferred from EGR. This problem is further aggravated by the EPA regulation known as SAPS (Sulfated Ash, Phosphorous and Sulfur) where chemical limits have been imposed on the amount of phosphorous (0.1 wt%), sulfur (0.12 wt%), sulfated ash (1 wt%) [2]. Since phosphorous and sulfur are major contributors in formation of anti-wear film in engine, their restriction would aggravate the wear of engine components in the diesel engine equipped with EGR protocols. This requires lubricating additives manufacturers to optimize their products to sustain the stringent and conflicting demands of chemical limits of main anti-wear elements while maintaining longer drain interval at the same time comply with EPA pollution norms.

Many studies have contributed significantly to understand this problem and various mechanisms have been proposed to explain the soot induced wear of diesel engine components equipped with EGR [1,3–34]. Although these mechanisms have contrasting explanation of the role played by soot to induce wear they have also established that the presence of soot degrades the lubrication oil properties physically and/or chemically.

Diesel engines operate under harsh conditions where presence of higher temperature and reactive decomposition products of lubricating oil increase the possibility of interaction between lubricating oil and soot. These interactions with reactive compounds might be responsible for adsorption of decomposition product on the soot structure. In addition, there also exists the possibility of modification in crystalline structure of diesel soot. Studies have suggested that three body wear condition are present when soot particles are trapped between two surfaces in relative motion [27]. Hence, it is possible that during three body wear, trapped diesel soot between two rubbing components experience extremely high local temperature and pressure that might induce modification in crystalline and/or amorphous domains of carbonaceous soot. It has also been shown that the higher hardness of soot particle compared to diesel engine component is another factor responsible for increased wear [27]. This higher surface hardness of the soot particles can possibly be due to changes in the turbostratic structure.

* Corresponding author.
E-mail address: aswath@uta.edu (P.B. Aswath).

0301-679X/$ - see front matter © 2012 Elsevier Ltd. All rights reserved.
http://dx.doi.org/10.1016/j.triboint.2012.03.004

Previous studies have demonstrated similarity in structure and morphology of various commercial carbon blacks and soot obtain from various sources such as coal, exhaust tail pipe, burner etc. [35,36]. Hence, In addition, the mechanism of synthesis of soot particle and carbon black particle also differs significantly. Soot is formed by high temperature pyrolysis of diesel fuel and its morphological parameters depend upon various combustion chamber parameters. On the other hand, carbon black has been manufactured by thermal oxidative decomposition of hydrocarbons and its morphological characteristics are controlled by choice of feedstock and process conditions [27,35,37,38]. This might induce some morphological differences between soot and carbon black. Hence BET nitrogen physisorption method has used to measure surface area of soot and carbon black. In the present study, a carbon black that has a turbostratic structure with a primary particle size of 30–50 nm was used for comparison.

Structure and morphology of "Exhaust Soot" obtained from tail pipe has been well documented [36,37,39]. but there is limited knowledge about soot recovered from crankcase oil. Hence, the objective of this study was to determine the structural, morphological and compositional characterization of crankcase soot and to examine the modification, if any. Energy dispersive X-ray spectroscopy (EDX) using transmission electron microscopy (TEM), bright field TEM together with selected area diffraction, X-ray photoelectron spectroscopy (XPS) and synchrotron X-ray diffraction and Raman spectroscopy were used to characterize the extracted soot.

This study is split into two parts. This paper details the structural, morphological and chemical characterization of diesel soot while the companion paper uses X-ray absorption near edge structure (XANES) spectroscopy to examine the local coordination of different chemical species in crankcase soot together with lattice imaging using high resolution transmission electron microscopy [40].

2. Experimental procedure

2.1. Diesel soot extraction

Used diesel engine oil was acquired from Freightliner diesel engine oil changing facility. The used engine oil was collected from the sump during the drain interval from a single diesel engine and was diluted using hexane as solvent in 50 wt% dilution. The mixture was centrifuged at 12,000 rpm for 2 h. The supernatant was discarded and remaining residue of soot was washed with hexanes, which was followed by centrifuging at 12,000 rpm for 2 h. This process was repeated three times which yielded a thick residue. To avoid the possibility of any trapped oil molecules a Soxhlet extraction method was used where extraction was carried out for 48 h using hexanes as solvent. The extracted soot was dried and lightly ground with a mortar and pestle to break up the large agglomorates which were formed during the extraction process.

2.2. Transmission electron microscopy

A JEOL 1200 EX STEM 120 kV, having a 0.34 nm point resolution, equipped with an EDAX Energy Dispersive X-ray spectrometer (EDS), was employed to study structure, morphology and composition of soot. Selected Area Diffraction Pattern (SADP) was used to probe structural information. SADP of diesel soot was compared with carbon black to determine possible structural change. EDS was used to acquire compositional information. Extracted soot was spread onto copper grid to load inside the TEM chamber for further characterization. High resolution transmission electron microscopy of the diesel soot was also conducted using a Hitachi H-9500 microscope operating at an accelerating voltage of 300 kV with a lattice resolution of 0.18 nm.

2.3. Surface area analysis

Surface area of the soot and carbon black were analyzed by the BET nitrogen physisorption method using an ASAP 2420 surface analysis and porosimetry instrument from Micrometrics Instrument Corporation instrument.

2.4. X-ray photoelectron spectroscopy

A Perkin-Elmer Phi 560 X-ray Photo-electron Spectroscopy was employed to probe compositional characterization of soot. XPS has also been employed to validate the results of EDX TEM. Al K_α X-ray ($h\nu = 1486.6$ eV) was used for excitation radiation operated at 14 kV and 300 W. The vacuum was maintained below 6×10^{-7} Torr during spectrum acquisition. A wide survey scan spectra was first acquired, followed by high resolution scans of P 1s, S 1s, Ca 1s and Zn 1s.

2.5. Raman spectroscopy

The Raman spectrometer used for the study was a Thermo scientific DXR spectrometer using diode pumped solid-state type laser as a source of illumination. The collection system was used in backscattered configuration. The samples were analyzed without any sample preparation by visualizing the sample using 10x microscope objective lens. To record the Raman spectra a solid-state laser was used with a frequency of 532 nm with maximum power output of 10 mW. It was necessary to use low laser power to avoid excessive sample heating. For this study a laser power of 1 mW was used. The laser spot diameter was 2 μm with 25 μm slit size, for the fully focused laser beam. The spectral resolution was 5 cm^{-1} at 532 nm with wavelength range from 50 cm^{-1} to 3500 cm^{-1}.

A dense layer of soot with a thickness of one millimeter was pressed with steel spatula onto a glass slide. This creates a macroscopically smooth surface. The sample holder is placed under a microscope and focused using white light. This white beam is then replaced with laser beam to acquire the spectra. Curve fitting for the determination of spectral parameters was performed with software program OriginLab. Curve fitting was executed by combination of various line shape. Best fit of the curve was accomplished without fixing or limiting the range of any spectral parameters during iteration.

2.6. X-ray diffraction and synchrotron X-ray diffraction

X-ray diffraction (XRD) patterns were collected both on a traditional laboratory diffractometer (Rigaku PMG, XRD lab at University of Trento) and at the MCX beamline at the Italian synchrotron radiation (SR) facility (ELETTRA at Trieste). The bending magnet beamline MCX has an energy range of 8–23 keV with an energy resolution ($\Delta E/E$) of 2×10^{-4} and a photon flux of 10^{11} photon/s.

The high brilliance and high angular resolution of synchrotron radiation (SR) allows identification and characterization of the minor components present on the soot. SR also allows photon energy tuning, therefore it is possible to perform measurements below and above the Zn absorption edge to better characterize the decomposition products, if any. SR X-ray diffraction of soot and carbon black were conducted at 9.4 keV and 10 keV which lie below and above the Zn K-absorption edge.

3. Results and discussion

3.1. Transmission electron microscopy

Transmission electron microscopy was employed to probe the structural, morphological and chemical composition of the extracted soot. Fig. 1(a) is a bright field transmission electron micrograph of the carbon black that shows primary particles that range in size from 20 nm to 50 nm in addition a few agglomerates in the size range of 200–500 nm are also present. These agglomerates are composed of collection of smaller basic particle units that are spherical or nearly spherical as shown in Fig. 1(a). Fig. 1(b) is the bright field TEM image of diesel soot which shows significant agglomeration of the primary particles, the agglomerates range in size from few hundred nanometers to some that are as large as 1 μm in size. However, the primary particles of diesel soot vary in diameter from 20 nm to 30 nm while primary particles of carbon black vary from 20 nm to 50 nm.

Significant research has been done to understand the internal structure and morphology of carbon black [41]. The primary particle is comprised of crystalline and amorphous domains. The crystalline domain is packed into hexagonal closed packed array, similar to graphite but in a turbostratic fashion. This graphite like crystalline domain typically consists of 3 and 4 graphene layers called platelets. Platelets are arranged in form of layer to make crystallites. Typically 4 and 5 platelets make crystallite with interlayer distance of about 3.5 Å which is regarded as highly disordered graphitic structure or turbostratic structure. Earlier studies have suggested the structural and morphological similarity between carbon black and soot obtained from various sources but with significant variation in particle size and agglomeration [36,41]. In addition, carbon black is predominantly carbonaceous ($>90\%$) and presence of other elements such as oxygen, hydrogen do not contribute to diffraction phenomena. Owing to these facts, carbon black has been used as reference material for comparison of structural changes in diesel soot.

Selected area diffraction in the TEM was used to probe the structure of carbon black and diesel soot. The SAD for carbon black is shown in Fig. 1(c) and that for diesel soot is shown in Fig. 1(d). Diffraction pattern of carbon black have three intense ring arising from (2 0 0) basal planes, (10) prism and (11) pyramidal planes. The diffraction patterns primarily arise from crystalline portion of the turbostratic structure. The *d*-spacing of the planes that give rise to the rings were calculated from the electron diffraction patterns and is shown in Table 1. In addition shown in the table are the ratios of the *d*-spacing. Close agreement in radii and radii ratio suggests that SAD of diesel soot is primarily originating from

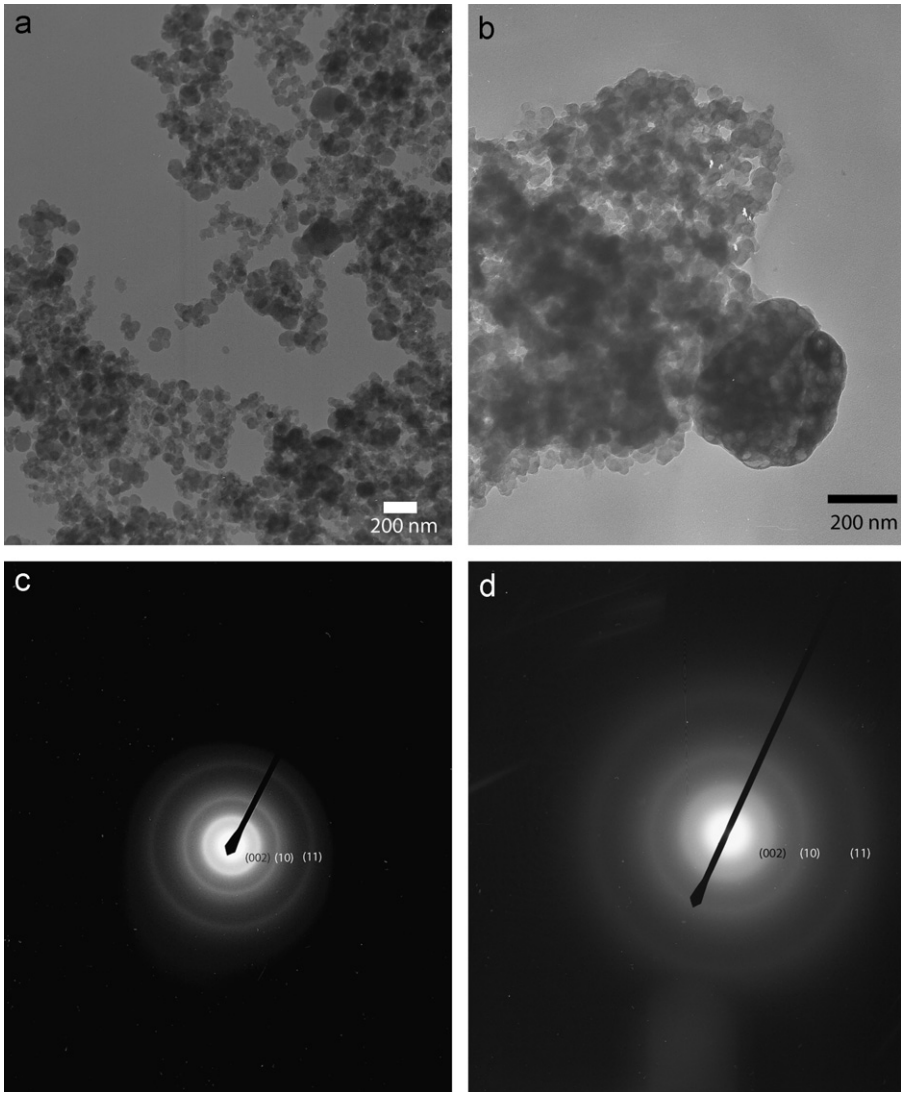

Fig. 1. (a) Bright field transmission electron micrograph of carbon black. (b) Bright field transmission electron micrograph of diesel soot, (c) selected area diffraction pattern of carbon black and (d) selected area diffraction pattern of diesel soot.

Table 1
d-spacing measurement for electron diffraction patterns for carbon black and diesel soot.

	1st ring *d*-spacing (R1)	**2nd ring *d*-spacing (R2)**	**3rd ring *d*-spacing (R3)**	**R2/R3**	**R1/R3**
Carbon black	0.361 nm (0 0 2)	0.209 nm (10)	0.121 nm (11)	1.71	2.93
Diesel soot	0.367 nm (0 0 2)	0.221 nm (10)	0.127 nm (11)	1.70	2.91

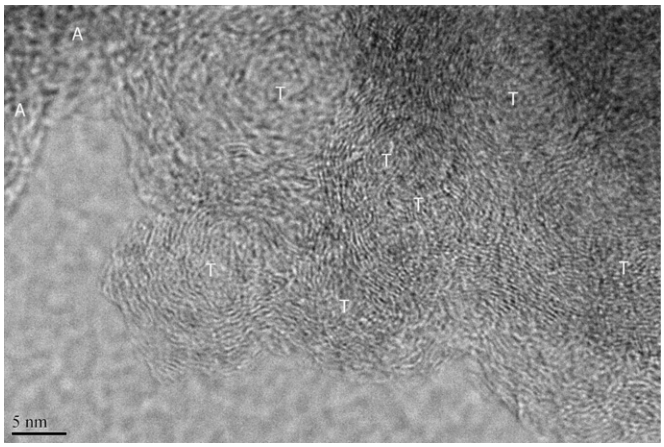

Fig. 2. High resolution bright field transmission electron micrograph of diesel soot showing turbostratic and amorphous regions.

crystalline domains of carbonaceous material of primary particles and is very similar to carbon black.

A detailed examination of the structure of soot was undertaken using high resolution transmission electron microscopy. Fig. 2 is a bright field HR-TEM image of diesel soot that clearly illustrates the turbostratic structure. Individual particles of the turbostratic structure range in size from 10 nm to 30 nm in diameter. The individual graphene layers are stacked atop each other in a circular fashion. Regions marked as *T* correspond to the turbostratic structure while regions marked *A* correspond to amorphous carbon. This structure is very similar to earlier studies conducted on carbon black [27]. This result suggests insignificant changes in the turbostractic structure of diesel soot due to interaction between lubrication additives.

Diesel soot is produced during the high temperature pyrolysis or combustion of hydrocarbon and is composed of primarily carbon and other elements such as hydrogen and oxygen are present in very small amounts [35]. One of the objectives of the present study was to understand the possibility of interaction between lubrication oil additives chemistries and diesel soot. Moreover, diesel soot experiences harsh diesel engine environment and reactive decomposition products of lubricating oil might change its chemical make up. Hence, Energy dispersive X-ray spectroscopy was used as a preliminary characterization tool to determine the chemical composition of diesel soot. EDS spectra were acquired from multiple regions of the soot including agglomerates as well as regions that contain dispersed turbostratic structure. Fig. 3(a) is from one of the agglomerated regions that show the presence of C from the turbostratic structure as well as presence of Ca, P, S, Zn and O. On the other hand spectra from a dispersed soot region shown in Fig. 3(b) shows primarily the presence of C with a little bit of O. Fig. 3(c) shows another EDS spectra from a small agglomerate that shows the presence of Ca, S, O and C but no P and Zn. The Cu peak in all three spectra originates from the copper grid used to mount the soot particles in the TEM stage.

It is well known fact that phosphorus, sulfur, zinc and calcium are main constituents of lubricating additive chemistry. It is worth noticing that, EDS could record the presence of phosphorus, sulfur, zinc and calcium only when electron beam was focused on bigger agglomerates while complete absence of such elements on smaller agglomerates was noticed. It was also observed that intensities of peak of phosphorous, sulfur, zinc & calcium differ on different agglomerates. In addition, some agglomerates shows presence of calcium and sulfur while phosphorus was absent in them. The multiple hexane wash and centrifuging of the oil coupled with Soxhlet extraction minimizes the presence of trapped engine oil in the agglomerates suggesting the presence of these elements originates from decomposition products of engine oil and/or wear debris from engine components.

Furthermore, the SAD from an region that contains agglomerates of soot particles, exhibits ring pattern originating from the smaller individual crystalline carbonaceous domains. In addition, phosphorous, sulfur, zinc and calcium that were detected by EDS are unlikely to be present on the soot structure particles in their elemental forms and more likely to be present as compounds and/or amorphous glassy structures. Amorphous compounds cannot be detected by SAD and we believe that a number of these crystalline compounds are very small and not always seen in traditional TEM. On the other hand, the $CaSO_4$ particles are quite large ($>1\ \mu m$) and are not shown here.

Surface area of the particles was measured using the BET nitrogen adsorption method indicated that carbon black has a surface area of 112.87 m^2/g and diesel soot has a surface area of 22.33 m^2/g. The difference in primary particle size for soot and carbon black are not very different, hence the large difference in surface area can be explained by the higher level of agglomeration in diesel soot in comparison to carbon black.

3.2. X-ray photoelectron spectroscopy

TEM – EDX results revealed the presence of P, S, Zn and Ca from the additive package incorporated into the diesel soot are most likely present as compounds and/or amorphous structures. In order to get better insight into these chemistries, X-ray photoemission spectroscopy was employed to examine the extracted soot. Fig. 4(a) and (b) show high resolution zinc and calcium spectra acquired using X-ray photoemission spectroscopy, respectively. Both spectra indicate a low signal to noise ratio indicative of the small amount of these elements present in soot. De-convoluted spectra of zinc suggest the presence of a peak at a binding energy 1023.05 eV which is binding energy of zinc 1s electron of zinc sulfate. De-convoluted spectra of calcium indicates the presence of a peak at 348.7 eV and 351.8 eV which represents the binding energy of calcium 1s electron of calcium sulfate and calcium oxide, respectively.

Previous studies have shown that $CaSO_4$ is due to the incorporation of overbased calcium sulfonates detergent additive in the tribofilms [42–44]. Hence, it is likely that the $CaSO_4$ may have come off as wear debris from the tribofilm and is embedded into soot agglomorate. The other possibility for the presence of calcium sulfate and calcium oxides may arise from the decomposed over based detergent, calcium sulfonates in the oil.

3.3. Raman spectroscopy

Raman spectroscopy is a promising characterization tool to investigate the short-range highly disordered graphitic structure.

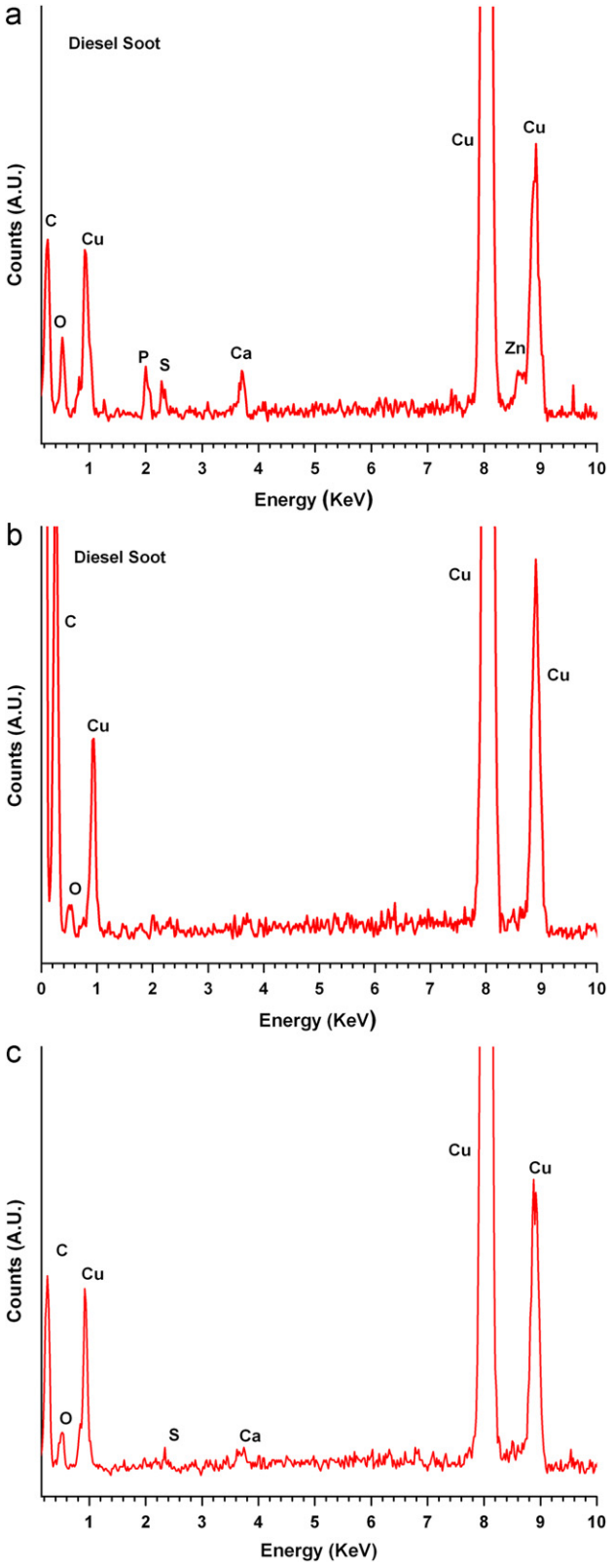

Fig. 3. (a) EDS spectra of diesel soot showing the presence of Ca, P, S, Zn, O and C in diesel soot. (b) EDS spectra of diesel soot showing the presence of C and O in diesel soot. (c) EDS spectra of diesel soot showing the presence of Ca, S, O and C in diesel soot.

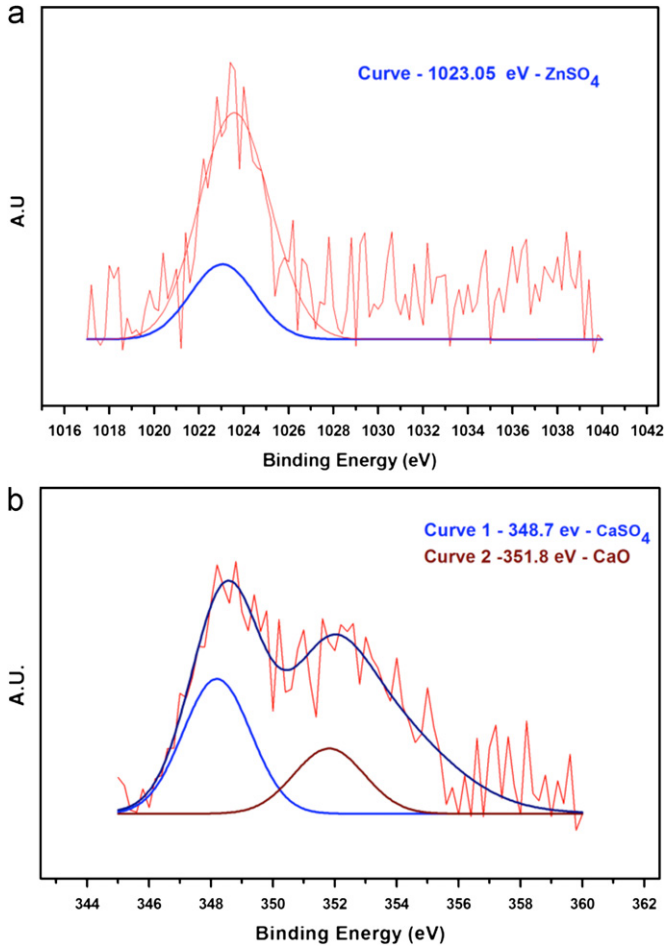

Fig. 4. (a) X-ray photoelectron spectoscopy high resolution spectra for zinc. (b) X-ray photoelectron spectoscopy high resolution spectra for calcium.

Earlier studies have shown that different types of soot could be distinguished based on the degree of graphitization. In addition, integrated intensity ratio of *D* and *G* peak is inversely proportional to microcrystalline planer size La that corresponds to the in-plane dimension of the single microcrystalline domain in graphite [45–49]. Valuable information can be obtained by analyzing different spectral features such as intensity, peak position, line shape and bandwidth between 800 cm^{-1} and 2000 cm^{-1}.

Fig. 5 shows the typical Raman spectra observed for diesel soot, carbon black and graphite acquired with a laser with λ=532 nm in the range 800–2000 cm^{-1}. The spectra exhibit two broad and strongly overlapping peak at intensity maxima ~1350 cm^{-1} and at ~1590 cm^{-1}. Previous studies revealed that the intensity maxima at ~1590 cm^{-1} (known as *G* band) is analogs to ideal graphitic vibration mode. Furthermore, increased degree of disorder in the graphite structure gives rise to the peak maxima at ~1350 cm^{-1} corresponds to disordered graphite. This peak is known as D1 peak (Defect bands).

The high signal intensity between the two peak maxima can be attributed to another band at ~1500 cm^{-1}, designated as *D*3(*A*) band which originates from the amorphous carbon fraction of soot (organic molecules, fragments or functional groups) and/or amorphous sp^2 bonded forms of carbon. Cuesta et al. [45] assumed Lorentzian line shape for this band, whereas Jawhari et al. [48] proposed Gaussian line shape due to a statistical distribution of amorphous carbon on interstitial places in the disturbed graphitic lattice of soot. Raman spectra recorded with λ=532 nm also exhibit second order spectra in the range of about 2300 cm^{-1} to 3300 cm^{-1}. For the given studies only first order spectra have been considered for further analysis.

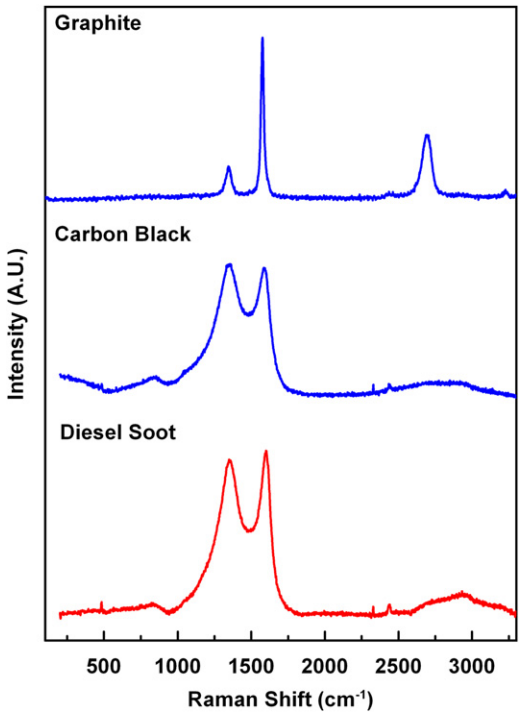

Fig. 5. Raman spectra of graphite, carbon black and diesel soot.

3.3.1. *Spectra analysis by curve fitting*

For the analysis and determination of spectral parameters by curve fittings various line shapes were evaluated. Raman spectra of diesel soot and carbon exhibit a broad band at about $\sim$1500 cm^{-1}. The band at 1500 cm^{-1} is associated with amorphous sp^2 bonded carbon. It is also worth taking into consideration that sp^3 bonded carbon have vibrational features frequency below 1500 cm^{-1}. This observation suggests the higher probability of sp^2 bonded amorphous carbons. The best fit was invariably achieved by either one or two combination of line shape for *G*, *D*1 and *D*3 peaks. One can use the Lorentz line shape for all three *G*, *D*1 and *D*3 peaks or one can use the Lorentzian line shape for *G* and *D*1 peak and Gaussian like shape for *D*3 peak. In this study we have used the Lorentzian peak fit for all three peaks of soot and carbon black as it offers the best fit. This fitting of the spectrum is in good agreement with recent studies by Sadezky et al. [46]. The polycrystalline graphite exhibits two sharp peaks at $\sim$1345 cm^{-1} and 1575 cm^{-1} that correspond to the *D*1 and *G* peak, respectively. The peak at $\sim$1500 cm^{-1} is not observed in graphite. The graphite with just the *D*1 and *G* peak was fitted with two Lorentzian curve fits. The curve fitted spectra of diesel soot, carbon black and graphite are show in Fig. 6((a)–(c)), respectively. For the carbon black a fourth peak was introduced in the fitting (*D*4) which takes into account for the disordered graphitic lattice due to polyenes and/or ionic impurities.

Further analysis of the spectra can be obtained by analyzing full width half maximum (FWHM) of the peaks, peak intensity and peak position. Table 2 details the curve fitted data and ratio of *G*/*D* peak intensity. The curve fitted spectral data reveals that for all samples FWHM of *G* peak is narrower than that of other two bands. This validates the fact that *G* peak corresponds to crystalline phase of carbon. Comparing the FWHM of graphite with diesel soot and carbon black, it evident that graphite has greater portion of crystalline phase. In addition, Table 2 breaks down the contribution from the different disordered forms of carbon including *D*1 the disordered graphitic lattice with contributions from graphene layer edges that are wrapped around, *D*3(*A*) the amorphous carbon and *D*4(*I*) arising from disordered graphitic layers from ionic impurities and polyenes. Overall the ratio of $G/(D1+D3+D4)$ for carbon black and diesel soot are very similar

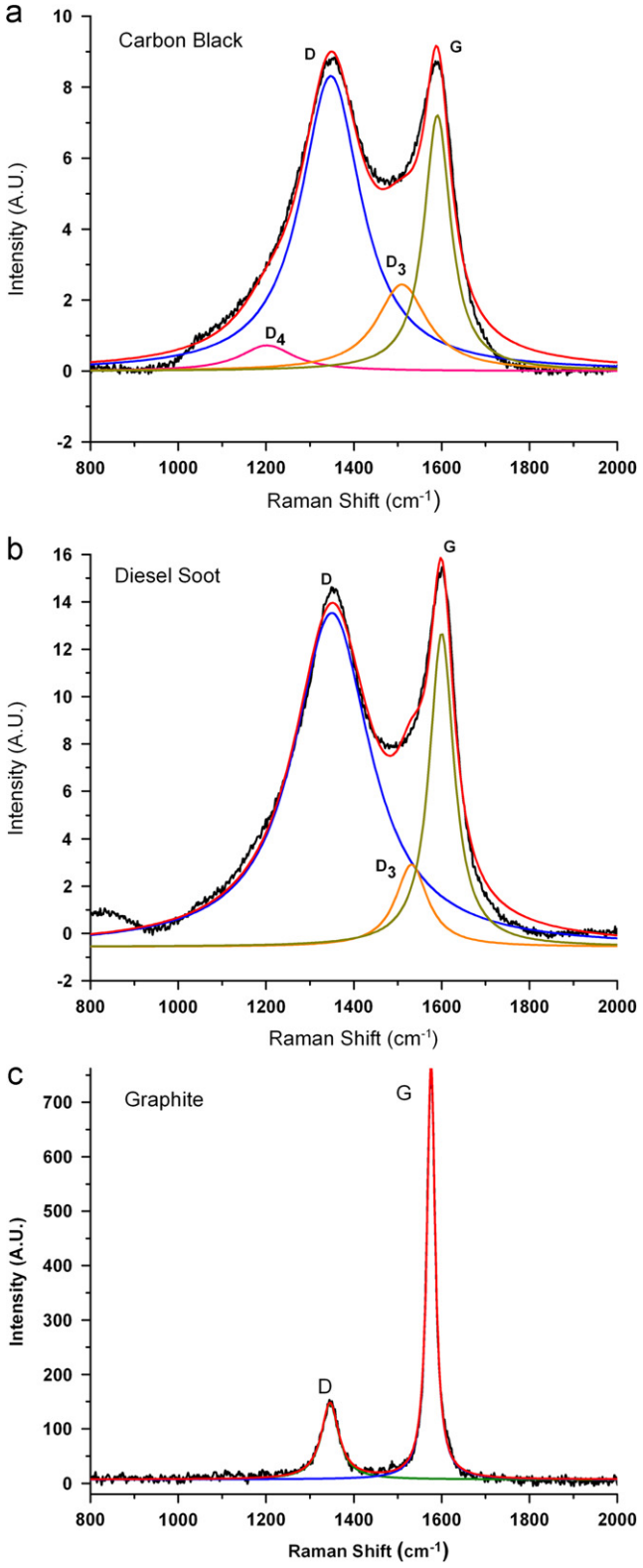

Fig. 6. (a) Deconvoluted Raman spectra of carbon black using Lorentzian curve fit for the *D*1, *D*3, *D*4 and *G* peaks. (b) deconvoluted Raman spectra of diesel soot using Lorentzian curve fit for the *D*1, *D*3 and *G* peaks. (c) Deconvoluted Raman spectra of graphite using Lorentzian curve fit for *D*1 and *G* peaks.

Table 2
Raman spectroscopic data for carbon black, diesel soot and graphite.

		Peak position	Intensity	*G*/*D*1	*G*/*D*3	*G*/*D*4	*G*/(*D*1+*D*3+*D*4)
Carbon black	*G*	1590.21	828.562	–	–	–	**0.29**
Carbon black	*D*1	1347.44	2171.804	**0.38**	–	–	
Carbon black	*D*3(*A*)	1509.39	534.336	–	**1.55**	–	
Carbon black	*D*4(*I*)	1201.96	169.469	–	–	**4.89**	
Diesel soot	*G*	1600.03	1402.114	–	–	–	**0.27**
Diesel soot	*D*1	1349.96	4683.579	**0.30**	–	–	
Diesel soot	*D*3(*A*)	1531.49	483.818	–	**2.90**	–	
Diesel soot	*D*4(*I*)	–	–	–	–	–	
Graphite	*G*	1575.80	27212.51	–	–	–	**2.55**
Graphite	*D*1	1345.64	10644.08	**2.55**	–	–	

G=Ideal graphitic lattice.
*D*1=Disordered graphitic lattice (graphene layer edges).
*D*3(*A*)=Amorphous carbon.
*D*4(*I*)=Disordered graphitic lattice, polyenes, ionic impurities.

suggesting a similar ratio of idealized graphite lattice and disordered carbon, however, a careful examination of the ratio's *G*/*D*1, *G*/*D*3 and *G*/*D*4 indicate some significant differences. The smaller *G*/*D*1 ratio for diesel soot indicates a larger proportion of graphene layer edges have reacted in soot resulting in a higher level of disorder. Other studies in functionalizing of graphene have shown that edges of the graphene layer may be functionalized more easily resulting in smaller *G*/*D*1 ratios [50]. This might be preferential location for reactive decomposition species for absorbtion. But more scientific investigation is required to validate the speculation. On the other hand *G*/*D*3 ratio for diesel soot is much smaller than the *G*/*D*3 ratio for carbon black indicating a smaller proportion of amorphous carbon in diesel soot compared to carbon black. Lastly, the absence of *D*4(*I*) peak in diesel soot indicates the absence of polyenes and/or other ionic impurities.

Although Raman spectra distinguishes the contribution from crystalline and amorphous domains no additional spectral features were observed to confirm contribution from interaction between lubrication additives chemistries and diesel soot.

3.4. XRD analysis of diesel soot

Synchrotron radiation X-ray diffraction was employed to acquire insight of interaction between lubrication additives chemistries and diesel soot and to validate results acquired from TEM EDX and XPS. Diesel-soot and carbon black X-ray diffraction patterns were collected on a traditional laboratory diffractometer (Rigaku IIID/max, XRD-lab at University of Trento, Trento, Italy) as well as at the MCX beamline (ELETTRA, the Italian synchrotron radiation facility at Trieste, Italy). Traditional laboratory diffractometer was used for initial assessment of composition of the soot which suggests the presence of calcium sulfate compounds. In addition, the earlier EDS analysis indicates the presence of Zn and P.

In order to determine the presence of Zn, synchrotron radiation X-ray diffraction was employed. Measurements were performed using different monochromatic wavelengths (energy) and patterns are shown in d^* (reciprocal space) scale in Fig. 7(a) and (b). Peaks at 0.43 and 0.5 correspond to the (1 1 1) and (2 0 0) planes originate from the aluminum sample holder used in synchrotron radiation (SR) XRD measurements. SR XRD measurements were made below (9.4 keV) and above (10 keV) the absorption edge of Zn (Zn *K*-edge is located at 9.6 keV). Any amorphous Zn phases, if present, would appear as increased background intensity in the spectra acquired with the SR beam with energy above the Zn *K* absorption edge. The diffraction spectra show considerable diffuse scattering signal that originates from turbostratic soot structure and from other incoherent scattering and fluorescence, which form the "background" signal. There also exist several Bragg peaks superposed on the diffused scattering background. These results indicate that in addition to the turbostratic structure various crystalline phases are also present in soot.

In order to distinguish the contribution from carbonaceous background of soot and contribution from crystalline phase, similar experiments were conduction on carbon black, as shown in Fig. 7(b). Electron diffraction study and the Raman analysis in the earlier sections indicate significant similarities between the carbon black and diesel soot and to a first approximation, it was assumed that the bulk of the background signal was coming from turbostratic structure of carbon black. In order to identify the nature of the crystalline peaks that appear to be superimposed on the large background peaks in diesel soot, the spectra from carbon black was subtracted from the spectra for diesel soot to yield a spectra for the crystalline phases as shown in Fig. 7(c). The spectra is superimposed for energy corresponds to above and below absorption of Zn *K* edge.

3.4.1. Fluorescence signal in the SR XRD measurements

From synchrotron measurements we can notice that diffuse scattering contribution (amorphous phase and fluorescence) is quite different between carbon black and diesel-soot. There are two possible explanations: (i) presence of a crystalline phase containing zinc and (ii) presence of an amorphous phase containing zinc. Measurements of carbon black were used as a blank to subtract the "background" signal, as shown in Fig. 7(c). The superimposed spectra above and below the Zn *K* absorption edge indicate no remarkable difference between the superimposed patterns that suggests absence of any zinc crystalline phases in the soot sample. Although, the specta after background subtraction using carbon black appear identical but considerable difference has been observed between the background signal from diesel soot and carbon black while changing energy from 9.4 keV to 10 keV. This strong effect in soot spectra above and below the absorption thresold of Zn *K* edge suggests the presence of zinc in amorphous form rather than any crystalline state.

3.4.2. Phase identification—search-match

In order to identify the crystalline phases present in diesel soot ICDD PDF4+ database of HighScore Search-Match software (Panalytical) was used. The spectra collected at 9.4 keV (SR XRD) with lowest diffuse scattering/ fluorescence and lower signal to noise ration was used for the phase identification.

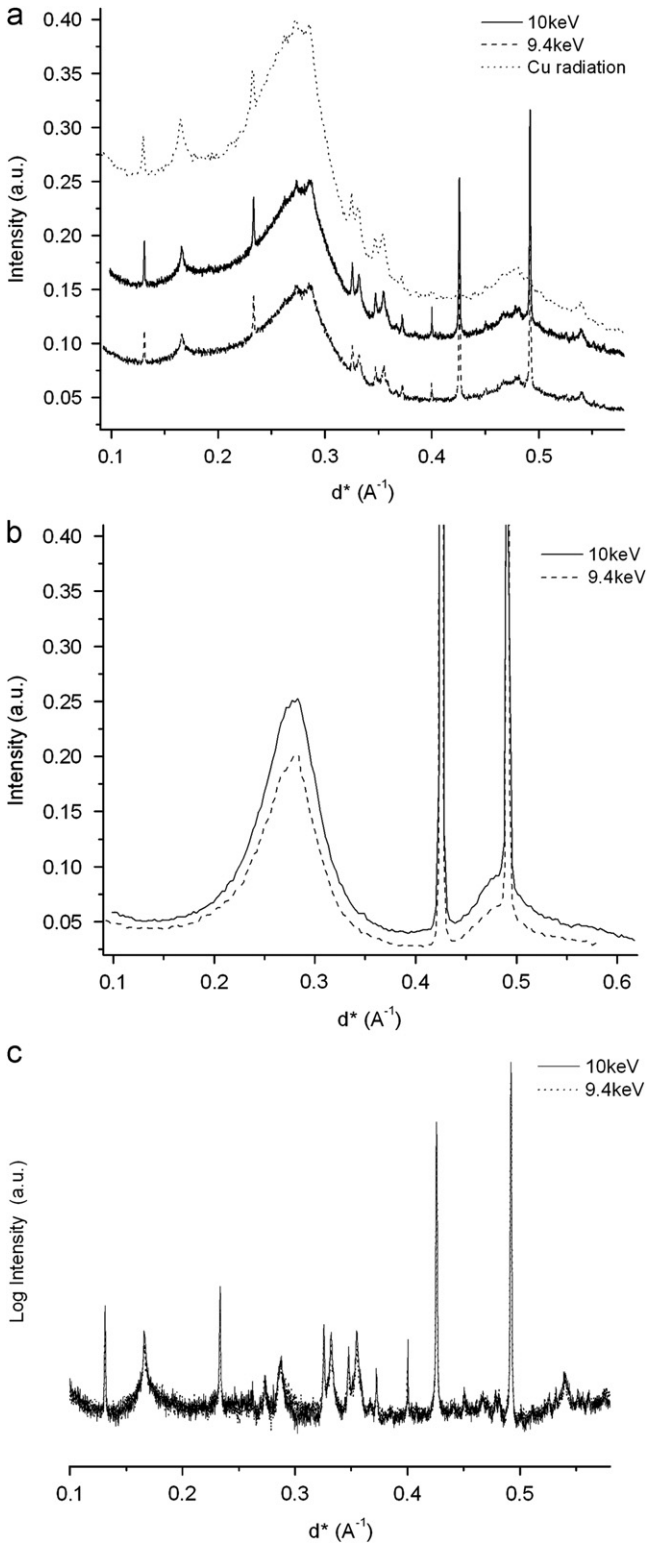

Fig. 7. (a) Conventional and synchrotron radiation X-ray diffraction spectra of diesel soot. Synchrotron X-ray spectra were acquired at 9.4 keV and 10 keV. (b) Synchrotron radiation X-ray diffraction spectra of carbon black with spectra acquired at 9.4 keV and 10 keV. (c) X-ray diffraction spectra of diesel soot after the spectra for carbon black was subtracted from it. Spectra correspond to acquisition energies of 9.4 keV and 10 keV. Spectra are plotted in terms of lattice spacing as they were acquired at different energies.

The search-match procedure was performed several times, using different constraints from the known chemical composition of metallic elements, namely, Ca, Zn (also Fe in some cases). Non-metallic elements considered were: H, C, O, S, P. Various speculated compounds such as CaO, $Ca(OH)_2$, $CaCO_3$, $CaSO_4$, $Zn_3(PO_4)_2$, $ZnSO_4$, ZnS were tried for search-match procedure.

Detailed analysis suggests that the most probable phases are different calcium sulfates in their hydrated phase. A good match were found with gypsum ($CaSO_4 \cdot 2H_2O$) and bassanite ($CaSO_4 \cdot 0.5H_2O$), respectively the dihydrate and hemihydrate phases. Fig. 8 is the SR X-ray diffraction spectrum from diesel soot that has been matched with known crystalline phases. From the observed pattern (after background removal), it is quite apparent that there is no CaO, $ZnSO_4$ or ZnS. Moreover, no Zn-containing phase shows unique matches (i.e., peaks attributed to a given phase only). On the contrary, two calcium sulfate hydrate phases gypsum (*G*) and bassanite (*B*) have unique matches, accounting for nearly all observed peaks. An additional (third) phase might be present, but it would be little justified: as an example, attempts to match other possible phases such as calcium hydrogen phosphate hydrate ($Ca_8H_2(PO_4)_6 \cdot 5H_2O$) and calcium hydrogen phosphite ($CaH_2O_5P_2$) were met with little success. It is also possible to add as a third phase as a Zn compound (zinc phosphate hydrate, $Zn_3(PO_4)_2 \cdot H_2O$), but no good match were found. All in all, we suggest the crystalline fraction to be made of gypsum and bassanite. The origin of these phases is likely from the detergent used in engine oil.

It is well known that overbased calcium sulfonates detergents are the primary detergents used in diesel engine oils, these detergents are made up of nanocrystalline $CaCO_3$ particles surrounded by micelle like calcium sulfonate ligands that keep $CaCO_3$ dispersed. The overbased detergents serve to neutralize acidic byproducts of combustion and help keep insoluble polar byproducts suspended in oil. The primary source of Ca in oil is the detergent while the source of sulfur is likely from a combination of the detergent as well as antiwear additives such as ZDDP and to smaller extent from the fuel source as well.

3.4.3. *Quantitative phase analysis*

If we assume the soot to be made of an amorphous matrix, with additional "background" signal from incoherent scattering and fluorescence, and two crystalline phases only (gypsum and bassanite), and considering also the contribution from the Al sample holder, the powder pattern of the soot measured using SR XRD can be used for a quantitative estimate of the crystalline phases. Since there is an "unknown" contribution form amorphous and other scattering terms, and also the sample holders cannot be quantified, the result of a Quantitative Phase Analysis (QPA) is just semi-quantitative, i.e., can be used to investigate the relative ratio between the two sulfate phases.

QPA was made using TOPAS, with standard structural data for gypsum and bassanite. The "background" signal was removed before the refinement. Al was added to account for the sample holder. With these data all diffraction peaks seem to be reasonably matched, apart from one line, at about 20.8°, which is apparently too strong for being matched by the given phases. So a free pseudo-Voigt peak function was added at that angle. Results from the semi-quantitative analysis indicates that the ratio of gypsum/bassanite = 0.5.

4. Discussion

In the present study structural, morphological and chemical characterization were conducted on extracted crackcase soot while the local coordination of the different elements in soot using XANES is detailed in the companion study [40]. The chemical characterization of crackcase soot using energy dispersive X-ray spectroscopy revealed the presence of phosphorous,

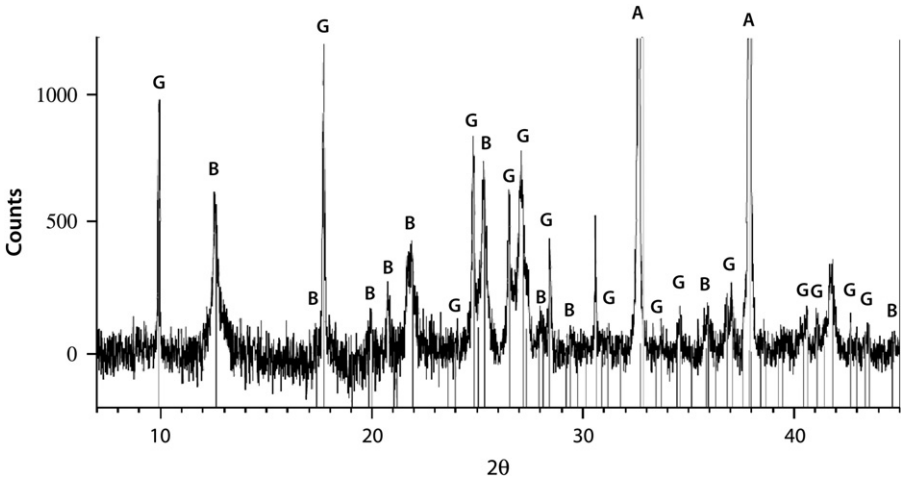

Fig. 8. X-ray diffraction spectra of crystalline constituents of diesel soot that have been indexed. *G* corresponds to gypsum ($CaSO_4 \cdot 2H_2O$), *B* corresponds to bassanite ($CaSO_4 \cdot 0.5H_2O$) and *A* corresponds to the Al sample holder.

sulfur, zinc and calcium on the larger agglomerates and complete absence of these elements on the individual primary particle of soot. Kawamura et al. used freeze fractal replica (FFR) method using TEM to investigate the state of soot in used diesel engine oil. He suggested that small soot particle in range of 0.02 μm do not affect the anti wear properties due to effectiveness of dispersant in engine oil on smaller particles. While particles greater than 0.03 μm might play dominant role in increase wear [51]. In similar studies, Narita et al. suggest soot with particle diameter equivalent to oil film thinkness between the cam nose and tappet shows possibilities of promoting wear [52]. Moreover, statistically designed experiments by Bardasz et al. studied the effect of dispersant level, dispersant type, oxidation level and detergent metal type on average roller follower shaft wear and viscocity growth and suggested that thickening oil is due to amount of soot and agglomerates rather than oxidative thickening [15,16]. These studies suggest that bigger agglomerates of soot induced higher wear but mechanism is poorly understood. In the present study, EDX results reveal the presence of phosphorus, sulfur, zinc and calcium on the agglomerates and their absence on the primary soot particle provide insight about this mechamism.

X-ray photoelectron spectroscopy results and synchrotron X-ray diffraction results substantiate EDX results as well as provide better insight about the various compounds present on the soot structure. XPS spectra have lower signal to noise ratio indicate the smaller concentration of the compunds on the soot structure. On the other hand, synchrotron X-ray diffraction uses high brilliance and intense photon flux to probe the samples. These results reveal the presence of crystalline calcium sulfate phase in its hydrated (gypsum) and hemishydrated (bassanie) form. In addition, synchrotron X-ray diffraction results also indicate the presence of zinc compound in the amorphous phase. These results also reveal the usefulness of 3rd generation synchrotron technique over tradional laboratory instrument to detect smaller concentrations of various compound present on soot. The particle size of the calcium sulfates detected by SR X-ray diffraction are much larger than the soot agglomorates and are typically 1–2 μm in size.

Furthermore, presence of crystalline calcium sulfate and amorphous zinc compounds on the soot structure could also orginate from decomposed reactive lubrication additives chemistries interacting with soot agglomorates. If these compounds orginates from decomposed reactive lubrication additives chemistries then it suggests interaction between reactive decomposition lubrication chemistries and diesel soot occurs during engine operation and/or in the oil sump. This phenomenon partially validates mechanism propsed by Round et al. where preferential adsorbtion of decomposed ZDDP was responsible for reduction in effectiveness of anti wear additives [9–12]. But further investigation is needed to probe the specific chemistries of zinc compounds and forms the basis of the companion study [40]. Previous studies also suggested the physical adosption of the decomposition chemistries on soot surfaces as a possible mechanism [9–12]. However, multiple washing, dilution, centrifuging followed by soxhlet extraction discard such possibilities of physical adsorption being the cause for the presence of these chemical species on diesel soot.

On the other hand, if the compounds originate from triofilm then it indicates interaction between trobofilm and soot. The mechanism, formation and structure of tribofilm have been well documented. Depending on the loading conditions, additives chemistries and other trobological conditions, tribofilm structure varies [53–60]. In general, ZDDP serve as protective anti wear additives by forming protection tribofilm under severe tribochemical reactions. These tribofilm primarily made up of short chain or long chain amorphous zinc poly phosphate depending on the severity of loading conditions and tests [42,57,61,62]. The presence of zinc based compounds in amorphous state in soot would suggest interaction between tribofilm and soot. In addition, previous studies have shown influence of overbased detergent chemistries on the structure of tribofilm [44,63–65]. They have shown that presence of overbased detergent chemistries form tribofilm made up of calcium sulfate and calcium phosphate. This might explain presence of crystalline phase of calcium sulfate as bassanite and gypsum on the soot structure. Hence, it can be postulated that three body wear which has been a model proposed in several [5,6,13,27,52] may be an important mechanism for the incorporation of amorphous phases of Zn and crystalline sulfates of calcium into the soot. The hardness of the amorphous Zn polyphosphates have been suggested to be as high as 20–30 GPa by Mosey et al. [55] in their molecular dynamic simulation studies and in experimental characterization of tribofilms it has been shown that hardness as high as 20 GPa have been measured by Aswath and co-workers [54,57]. The hardness of the steel substrate is typically in the range of 7–8 GPa and it is conceivable that presence of hard amorphous polyphosphates of Zn may contribute to third body wear. On the other hand both, bassanite and gypsum have a hardness of 2 on the Moh's scale, just above talc and not likely the source of any abrasive wear in diesel engines.

Strutucal characterization of crankcase soot using selected area diffraction in a TEM suggest insignificant changes in the turbostratic structure of soot in comparion to carbon black.

Raman spectroscopy used to probe short-range disorder structure of soot and carbon black indicates that the ratio of $G/(D1+D3+D4)$ peaks for carbon black and diesel soot are very similar suggesting a similar ratio of idealized graphite lattice and disordered carbon, however, a careful examination of the ratio's $G/D1$, $G/D3$ and $G/D4$ indicate some significant differences. Although Raman spectra distinguish the contribution from crystalline and amorphous domains but no additional spectral features were observed to confirm contribution from interaction between lubrication additives chemistries and diesel soot using Raman spectroscopy.

5. Conclusions

Diesel soot was extracted from used engine oil by dilution with hexanes followed by centrifuging and soxhlet process. The morphology, structure, morphology and chemistry of diesel soot was characterized and compared to carbon black using transmission electron microscopy, Raman spectroscopy and synchrotron X-ray diffraction.

(i) Transmission electron microscopy of both carbon black and diesel soot indicate that both of them exhibit a turbostratic structure with identical spacings of the (0 0 2), (10) and (11) pattern. The primary particle size of carbon black is in the 20–50 nm range while that of diesel soot is 20–30 nm. However, diesel soot has larger agglomorates compared to carbon black.

(ii) Energy dispersive spectroscopy of the diesel soot in the transmission electron microscopy yielded different compositions based on location of acquisition. Larger agglomorates exhibited the presence of P, S, Ca, Zn, C and O while EDS of individual particles yielded only C and O. In addition, some regions showed only the presence of Ca, S, C and O.

(iii) Raman spectroscopy of carbon black and diesel soot exhibited several similarities, but also some distinctive differences. Both spectra exhibited the presence of ordereded and disordered carbon with the overall ratio of ordered to disordered structure being similar. Diesel soot appeared to contain a larger proportion of graphene layer edges in comparison to carbon black that had a higher proportion of ionic impurities.

(iv) Synchrotron X-ray diffraction of the soot indicated the presence of crystalline peaks superimposed on the background pattern from the turbostratic structure. Subtraction and quatification of the crystalline contribution to the spectra indicated the presence of gypsum and bassanite (allotrophs of $CaSO_4$) in the ratio of 1:2.

(v) Examination of the synchrotron X-ray diffraction spectra acquired at 9.4 keV and 10 keV on either side of the Zn *K*-absorption edhe indicated higher background absorption suggesting that Zn containing species while absent as crystalline peaks are present in their amorphous state.

Acknowledgment

This research was partially conducted when one of the investigators (P.B. Aswath) was on a Fulbright Faculty Fellowship in Univeristy of Trento. Synchrotron X-ray diffraction was conducted at the MCX beamline at ELETTRA in Trieste, Italy. Raman and transmission electron microscopy were conducted at Center for Characterization for Materials and Biology at University of Texas at Arlington.

References

[1] Aldajah S, Ajayi OO, Fenske GR, Goldblatt IL. Effect of exhaust gas recirculation (EGR) contamination of diesel engine oil on wear. Wear 2007;263(1-6):93–8.
[2] Lawrence LG. Heavy-duty diesel engine oil developments and trends. Machinery Lubrication 〈http://www.machinerylubrication.com/Read/1036/diesel-engine-oil〉 May 2007.
[3] Sasaki M, Kishi Y, Hyuga T, Okazaki K, Tanaka M, Kurihara I. Effect of EGR on diesel engine oil, and its countermeasures. Proceedings of the 1997 International Spring Fuels & Lubricants Meeting, May 5, 1997–May 8 1997;1271: 39–44.
[4] Nagai I, Endo H, Nakamura H, Yano H. Soot and valve train wear in passenger car diesel engines. SAE Technical Paper 8317,57, 1983.
[5] Kuo CC, Passut CA, Jao T, Csontos AA, Howe JM. Wear mechanism in Cummins M-11 high soot diesel test engines. Proceedings of the 1998 SAE International Spring Fuels & Lubricants Meeting & Exposition, May 4, 1998–May 6 1998;1368: 21–32.
[6] Mainwaring R. Soot and wear in heavy duty diesel engines. Proceedings of the 1997 International Spring Fuels & Lubricants Meeting, May 5, 1997–May 8 1997;1273: 47–63.
[7] McGeehan JA, Rynbrandt JD, Hansel TJ. Effect of oil formulations in minimizing viscosity increase and sludge due to diesel engine soot. SAE TechnicalPaper 841370,1984.
[8] Ratoi M, Castle RC, Bovington CH, Spikes HA. The influence of soot and dispersant on ZDDP film thickness and friction. Lubrication Science 2004;17:25–43.
[9] Rounds FG. Effect of lubricant additives on the prowear characteristics of synthetic diesel soots. Lubrication Engineering 1987;43:273–82.
[10] Rounds FG. Generation of synthetic diesel engine oil soots for wear studies. Lubrication Engineering 1984;40:394–401.
[11] Rounds FG. Soots from used diesel engine oils—their effects on wear as measured in 4-ball wear tests. SAE Technical Paper 810499,1981.
[12] Rounds FG. Carbon: cause of diesel engine wear? SAE Technical Paper No. 770829, 1977.
[13] Yamaguchi ES, Utermann M, Roby SH, Ryason SH, Yeh SW. Soot wear in diesel engines. Proceedings of the Institution of Mechanical Engineers, Part: Journal 2006;220:463–9.
[14] Akiyama K, Masunaga K, Kado K, Yoshioka T. Cylinder wear mechanism in an EGR-equipped diesel engine and wear protection by the engine oil. SAE Technical Paper No. 872158, 1987.
[15] Bardasz EA, Carrick VA, Ebeling VL, George HF, Graf MM, Kornbrekke RE. Understanding soot mediated oil thickening through designed experimentation—Part 2: GM 6. 5 L.Proceedings of the 1996 International Fall Fuels & Lubricants Meeting & Exposition, October 14, 1996–October 17 1996; 1210:57–68.
[16] Bardasz EA, Carrick VA, George HF, Graf MM, Kornbrekke RE, Pocinki SB. Understanding soot mediated oil thickening through designed experimentation—Part 5: Knowledge exhancement in the GM 6. 5 L. Proceedings of the 1997 International Fall Fuels & Lubricants Meeting & Exposition, October 13, 1997–October 16, 1997; 1304:126–140.
[17] Berbezier I, Martin JM, Kapsa P. Role of carbon in lubricated mild wear. Tribology International 1986;19:115–22.
[18] Castillo C, Spikes HA. The behavior of diluted sooted oils in lubricated contacts. Tribology Letters 2004;16:317.
[19] Colacicco P, Mazuyer D. Role of soot aggregation on the lubrication of diesel engines. Tribology Transactions 1995;38:959–65.
[20] Corso S, Adamo R. Incipient scuffing detection by ferrography in a diesel valve train system. Engine Lubrication. International Fuels and Lubricants Meeting and Exposition., Tulsa, Oklahoma, USA., October 21–24, 1985: 33–49.
[21] Corso S, Adamo R. Effect of diesel soot on reactivity of oil additives and valve train materials. SAE Technical Paper No. 841369,1984.
[22] Dennis AJ, Garner CP, Taylor DHT. The effect of EGR on diesel engine wear. SAE Technical Paper No. 1999-01-0839, 1999.
[23] Gautam M, Chitoor K, Durbha M, Summers JC. Contribution of soot contaminated oils on engine wear—investigation of novel oil formulations. Tribology International 1999;32(12):697–9.
[24] Hirose Y, Kunoki T. Recent studies on diesel soot and valve train wear. Journal of Japan Society of Lubrication Engineers 1987;32:159–64.
[25] Hirose Y, Kunoki T, Kawashima K, Kanai S, Hirami K. Development of a new multigrade engine oil for improved wear resistance in heavy vehicle diesel engines—Part I: Diesel soot and valve train wear. SAE Technical Paper No. 852134,1985.
[26] Hosonuma K, Yoshida K, Matsunaga A. Decomposition products of zinc dialkydithiophosphate in an engine and their interaction with diesel soot. Wear 1985;103:297–309.
[27] Jao T-C, Li S, Yatsunami K, Chen SJ, Csontos AA, Howe JM. Soot characterisation and diesel engine wear. Lubrication Science 2004;16:111–26.
[28] Kagaya M. Study on diesel soot Part 1: Effect of diesel soot on valve train wear in passenger car diesel engines. Journal of the Japan Petroleum Institute 1997;40:482–7.
[29] Kagaya M. Study on diesel soot Part 2: Discussion concerning the mechanism of valve train wear by diesel soot. Journal of the Japan Petroleum Institute 1997;40:488–93.

[30] Kagaya M, Kagawa T, Takahashi Y. Study on diesel soot Part 3: A new proposal on the mechanism of wear promoted by soot. Journal of the Japan Petroleum Institute 1997;40:494–9.
[31] Kaneta M, Irie T, Nishikawa H, Matsuda K. Effects of soot on wear in elastohydrodynamic lubrication contacts. Proceedings of the Institution of Mechanical Engineers, Part: Journal 2006;220:307–17.
[32] Kano M, Tanimoto I, Nakamura K, Fujiki A. Effect of the EGR system on valve train wear in diesel engine. Journal of JSLE International Edition 1988:133–8.
[33] Kawamura M, Ishiguro T, Fujita K, Morimoto H. Deterioration of antiwear properties of diesel engine oils during use. Wear 1988;123(3):269–80.
[34] Kimijima T, Haneishi T, Okabe H. Effect of soot on anti-wear properties of marine diesel engine oils. Journal of Japanese Society of Tribologists 1994;39: 337.
[35] Lahaye J. Mechanisms of soot formation. Polymer Degradation and Stability 1990;30:111–21.
[36] Clague ADH, Donnet JB, Wang TK, JCM Peng. Comparison of diesel engine soot with carbon black. Carbon 1999;37(10):1553–65.
[37] Mikhailov EF, Vlasenko SS, Ryshkevitch TI, Kiselev AA. Soot structure investigation: adsorptional properties. Journal of Aerosol Science 1996;27(1): 709–710.
[38] Prado G, Lahaye J, Haynes BS. Soot particle nucleation and agglomeration. Soot in Combustion Systems and its Toxic Properties—Proceedings of a NATO Workshop on Soot in Combustion Systems. 1983; 7:145-161.
[39] Tumolva L, Park J, Kim J, Miller AL, Chow JC, Watson JG, Park K. Morphological and elemental classification of freshly emitted soot particles and atmospheric ultrafine particles using the TEM/EDS. Aerosol Science and Technology 2010;44: 202–215.
[40] Patel M, Aswath PB. Morphology, structure and chemistry of extracted diesel soot: Part II: High resolution transmission electron microscopy, X-ray absorption near edge structure spectroscopy. Tribology International 2012. http://dx.doi.org/10.1016/j.triboint.2012.02.022.
[41] Donnet JB. Carbon Black: Science and Technology. New York: Marcel Dekker, Inc; 1993.
[42] Nehme G, Mourhatch R, Aswath PB. Effect of contact load and lubricant volume on the properties of tribofilms formed under boundary lubrication in a fully formulated oil under extreme load conditions. Wear 2010;268(9-10):1129–47.
[43] Costello MT, Urrego RA. Study of surface films of the ZDDP and the MoDTC with crystalline and amorphous overbased calcium sulfonates by XPS. Tribology Transactions 2007;50:217–26.
[44] Costello MT, Kasrai M. Study of surface films of overbased sulfonates and sulfurized olefins by X-Ray absorption near edge structure (XANES) spectroscopy. Tribology Letters 2006;24:163–9.
[45] Cuesta A, Dhamelincourt P, Laureyns J, Martinez-Alonso A. Tascon JMD. Raman microprobe studies on carbon materials. Carbon 1994;32:1523–32.
[46] Sadezky A, Muckenhuber H, Grothe H, Niessner R, Poschl U. Raman microspectroscopy of soot and related carbonaceous materials: spectral analysis and structural information. Carbon 2005;43:1731–42.
[47] Escribano R, Sloan JJ, Siddique N, Sze N, Dudev T. Raman spectroscopy of carbon-containing particles. Vibrational Spectroscopy 2001;26:179–86.
[48] Jawhari T, Roid A, Casado J. Raman spectroscopic characterization of some commercially available carbon black materials. Carbon 1995;33:1561–5.
[49] Gruber T, Zerda TW, Gerspacher M. Raman studies of heat-treated carbon blacks. Carbon 1994;32:1377–82.
[50] Sharma R, Baik JH, Perera CJ, Strano MS. Anomalously large reactivity of single graphene layers and edges toward electron transfer chemistries. Nano Letters 2010;10:398–405.
[51] Kawamura M, Ishiguro T, Fujita K, Hidetake M. Deterioration of antiwear properties of diesel engine oils during use. Wear 1988;123:269–80.
[52] Narita K. Effects of diesel soot on engine oil performance. Journal of Japanese Society of Tribologists 1997;42:425–9.
[53] Huq MZ, Aswath PB, Elsenbaumer RL. TEM studies of anti-wear films/wear particles generated under boundary conditions lubrication. Tribology International 2007;39:111–6.
[54] Mourhatch R, Aswath PB. Nanoscale properties of tribofilms formed with zinc dialkyl dithiophosphate (ZDDP) under extreme pressure condition. Journal of Nanoscience and Nanotechnology 2008;9:2682–91.
[55] Nicholas JMosey, Martin HMüser, Tom KWoo. Molecular mechanisms for the functionality of lubricant additives. Science 2005;307(5715):1612–5.
[56] Mourhatch R, Aswath PB. Tribological behavior and nature of tribofilms generated from fluorinated ZDDP in comparison to ZDDP under extreme pressure conditions—Part 1: Structure and chemistry of tribofilms. Tribology International 2011;44:187–200.
[57] Mourhatch R, Aswath PB. Tribological behavior and nature of tribofilms generated from fluorinated ZDDP in comparison to ZDDP under extreme pressure conditions—Part II: Morphology and nanoscale properties of tribofilms. Tribology International 2011;44:201–10.
[58] Fujita H, Spikes HA. The formation of zinc dithiophosphate antiwear films. Proceedings of the Institution of Mechanical Engineers, Part: Journal J 2004;218:265–77.
[59] Spikes HA. The history and mechanisms of ZDDP. Tribology Letters 2004;17:469–89.
[60] Topolovec-Miklozic K, Forbus TR, Spikes HA. Film thickness and roughness of ZDDP antiwear films. Tribology Letters 2007;26:161–71.
[61] Nicholls MA, Norton PR, Bancroft GM, Kasrai M, Do T, Frazer BH, et al. Nanometer scale chemomechanical characterization of antiwear films. Tribology Letters 2004;17:205–16.
[62] Nicholls MA, Norton PR, Bancroft GM, Kasrai M. X-ray absorption spectroscopy of tribofilms produced from zinc dialkyl dithiophosphates on Al–Si alloys. Wear 2004;257:311–28.
[63] Yu LG, Yamaguchi ES, Kasrai M, Bancroft GM. The chemical characterization of tribofilms using XANES—interaction of nanosize calciumcontaining detergents with zinc dialkyldithiophosphate. Canadian Journal of Chemistry 2007;85:675–84.
[64] Selby K, Urbanak M, Leonhardt H, Colbourne D, Burnett P, Machatschek F et al. Meeting the lubrication challenges of heavy duty low emission diesel engines. World Tribology Congress III, September 12, 2005–September 16, 2005: Paper No. WTC2005-63983:547–8.
[65] Yin Z, Kasrai M, Bancroft GM, Fyfe K, Colaianni ML, Tan KH. Application of soft x-ray absorption spectroscopy in chemical characterization of antiwear films generated by ZDDP—Part II: The effect of detergents and dispersants. Wear 1997;202:192–201.